Insect Biochemistry and Molecular Biology 43 (2013) 1009–1014

Contents lists available at ScienceDirect

Insect Biochemistry and Molecular Biology

journal homepage: www.elsevier.com/locate/ibmb

Regulation of atrophin by both strands of the mir-8 precursor

Mercedes Rubio [a], Raúl Montañez [a], Lidia Perez [b], Marco Milan [b], Xavier Belles [a,*]

[a] Institute of Evolutionary Biology (CSIC – Universitat Pompeu Fabra), Passeig Maritim de la Barceloneta 37, 0803 Barcelona, Spain
[b] Institute for Research in Biomedicine (IRB Barcelona), Baldiri Reixac 10, 08028 Barcelona, Spain

ARTICLE INFO

Article history:
Received 1 July 2013
Received in revised form
2 August 2013
Accepted 8 August 2013

Keywords:
Atrophin
miR-8
Argonaute
miRNA passenger strand
Blattella
Drosophila
Metamorphosis

ABSTRACT

In *Drosophila melanogaster*, miR-8-3p regulates mRNA levels of atrophin, a factor involved in neuromotor coordination, and we found that *Blattella germanica* with suppressed atrophin showed motor problems. Bionformatic predictions and luciferase-reporter tests indicated that *B. germanica* atrophin mRNA contains target sites for miR-8-3p and miR-8-5p. Suppression of miR-8-3p or miR-8-5p appeared to increase atrophin mRNA. The effects of suppression of Argonaute (AGO) 1 or AGO2 expression on miR-8-3p and miR-8-5p suggested that miR-8-3-p might predominantly bind to AGO1, whereas miR-8-5p might bind to a moderate extent to both AGO1 and AGO2 in the respective RNA-induced silencing complexes (RISCs). We propose that the interplay of miR-8-3p, miR-8-5p, AGO1 and AGO2, maintain the appropriate levels of atrophin mRNA. This would be the first example of two strands of the same miRNA precursor regulating a single transcript.

1. Introduction

One of the most relevant recent advances in the field of regulation of gene expression is the discovery of microRNAs (miRNAs) in the nematode *Caenorhabditis elegans* (Lee et al., 1993). Subsequently, the occurrence of miRNAs has been reported in almost all animal and plant groups (Griffiths-Jones et al., 2008) and their role as key protagonists of an additional layer of regulation of gene expression is now widely recognized (Bartel, 2004). Today, miRNAs can be defined as endogenous short noncoding RNAs of 21–23 nucleotides that generally regulate a target mRNA by blocking its translation and even by degrading it. With this mechanism, miRNAs sculpt mRNA and protein patterns, confer robustness to biological processes by refining transcriptional programs and attenuating aberrant transcripts, and may help to suppress random fluctuations in transcript copy number. For these reasons, miRNAs have been qualified as "fine-tuning" molecules (Bartel, 2004), and their importance has been recognized not only in normal development and physiology, but also in medical sciences and in evolution (Christodoulou et al., 2010; Ebert and Sharp, 2012).

Mature miRNAs are processed from the corresponding hairpin miRNA precursor by the RNase III enzyme Dicer yielding two partially complementary single strand miRNAs: the "mature" miRNA and the "passenger" strand (Kim et al., 2009). In insects, the so-called mature miRNA is generally incorporated into the RNA-induced silencing complex (RISC) combined with the protein Argonaute (AGO) 1, which has endonuclease activity directed against mRNA strands that display extensive complementarity to their bound miRNA. The miRNA then guides the AGO1-RISC to the target mRNA, binds to the imperfectly-paired miRNA sites located within it, and blocks transcript translation, eventually leading to mRNA degradation, according to the typical mode of action of miRNAs (Bartel, 2004; Belles et al., 2012). The so-called passenger strand is generally degraded, but in some cases it can be incorporated into a AGO2-RISC, which is optimized for target mRNA degradation (Czech et al., 2009; Okamura et al., 2009).

In an 11-million reads miRNA library from whole-body sixth instar female nymphs of the cockroach *Blattella germanica*, we noticed a number of cases where the "passenger" strand of a given miRNA was as abundant, or even more abundant, than the corresponding "mature" miRNA (Cristino et al., 2011), which suggested that the two strands of the same precursor give functional miRNAs. This was not surprising, given that previous investigations in vertebrates (Yang et al., 2011) and in the fly *Drosophila melanogaster* (Okamura et al., 2008) had shown that a significant number of "passenger" miRNAs are structurally conserved in diverse animal groups, suggesting that they function as miRNAs. In our miRNA library, the case of miR-8 was of particular interest because the

* Corresponding author. Tel.: +34 932309636; fax: +34 932309555.
E-mail address: xavier.belles@ibe.upf-csic.es (X. Belles).

0965-1748/$ – see front matter © 2013 Elsevier Ltd. All rights reserved.
http://dx.doi.org/10.1016/j.ibmb.2013.08.003

"mature" miR-8 (actually, miR-8-3p) was represented by 4906 reads, whereas for the "passenger" strand (miR-8-5p), 47,160 reads were counted (Cristino et al., 2011). In *D. melanogaster*, miR-8-5p is also highly expressed, but the relative expression levels are still 40-fold higher in the case of miR-8-3p (Berezikov et al., 2011). The question that intrigued us was whether miR-8-5p might function as a miRNA in *B. germanica*.

A search for miR-8 target candidates in insects revealed a paper by Stephen Cohen and his coworkers (Karres et al., 2007) who elegantly demonstrated that miR-8 (indeed, miR-8-3p) regulates mRNA levels of atrophin in *D. melanogaster*. *Drosophila* atrophin is related to the atrophin family of mammalian transcriptional co-repressors that play key roles in developmental and neural processes (Wang and Tsai, 2008). Cohen's team identified *Drosophila* atrophin as a direct target of miR-8-3p, and showed that mutant miR-8-3p phenotypes had high atrophin activity, which resulted in elevated brain apoptosis and in neuromotor coordination defects (Karres et al., 2007). With these antecedents, we proceeded with our cockroach model by cloning and characterizing, in structural and functional terms, the cDNA or RNA corresponding to the main players that might be involved in the above process in question: atrophin, the miR-8 precursor and its two strands miR-8-3p and miR-8-5p, and the associated AGO1 and AGO2 proteins.

2. Materials and methods

2.1. Insects

Freshly ecdysed sixth (last) instar nymphs of the cockroach *B. germanica* were obtained from a colony reared in the dark at 30 ± 1 °C and 60–70% relative humidity. The entire animal except the head (to avoid interferences with the eye pigments) and the digestive tube (to avoid contamination with parasites) was used for RNA extractions. All dissections were carried out on carbon dioxide-anaesthetized individuals. Samples for RNA extraction and quantification were frozen immediately after dissection, and stored at −80 °C until use. RNA isolation was carried out with miRNeasy® Mini Kit (QIAGEN), which increases the yield of small RNAs. Reverse transcription was carried out with the NCode™ miRNA First-Strand cDNA Synthesis and qRT-PCR Kits (Invitrogen), which allows the quantification of large and small RNAs by real-time PCR.

2.2. Cloning the miR-8 precursor

Using the sequences of miR-8-5p and miR-8-3p as primers and cDNA from last instar female nymphs of *B. germanica* as template, we amplified a fragment of 59 bp, which was subcloned into the pSTBlue-1 vector (Novagen) and sequenced. The RNA fold algorithm of Gruber et al. (2008) was used to predict if the primary sequences obtained folded following the typical hairpin structure of a pre-miRNA.

2.3. Cloning atrophin cDNA

A partial sequence of *B. germanica* atrophin, including the 3′UTR, was obtained following a RT-PCR strategy using degenerate primers designed on the basis of conserved motifs from insect atrophin sequences and cDNA from last instar female nymphs of *B. germanica* as a template. The sequence of the amplified fragment (973 bp) was identified as the equivalent region in known insect atrophin sequences. Then, the 3′ fragment of the sequence was completed by 3′ RACE (3′-RACE System Version 2.0; Invitrogen) using the same template, thus obtaining a final fragment of 1820 bp (GenBank accession number HF912426). PCR products were subcloned and sequenced as described above. Primer sequences are indicated in the Table S1.

2.4. Cloning AGO1 and AGO2 cDNAs

The *B. germanica* AGO1 and AGO2 were obtained following a RT-PCR strategy using specific primers based on sequences obtained from *B. germanica* transcriptomes of whole body of sixth instar female nymph, and cDNA from the same instar and sex as template. We further extended the sequence by subsequent 3′ and 5′ RACEs using cDNA from last instar female nymphs, and we obtained a sequence of 2834 bp length for AGO1 and of 3361 bp length for AGO2 (GenBank accession numbers HF912424 and HF912425, respectively). PCR products were subcloned into the pSTBlue-1 vector (Novagen) and sequenced. Primer sequences are indicated in the Table S1.

2.5. Quantification of miRNAs and mRNAs by quantitative real-time PCR

For miRNA and mRNA expression studies by quantitative real-time PCR (qRT-PCR), 400 ng of total RNA were reverse transcribed using the NCodeTM First-Strand cDNA Synthesis Kit (Invitrogen), which works for both miRNA and mRNA quantification, following the manufacturer's protocols. Amplification reactions were carried out using IQTM SYBR Green Supermix (BioRad) and the following protocol: 95 °C for 2 min, and 40 cycles of 95 °C for 15 s and 60 °C for 30 s, in a MyIQ Real-Time PCR Detection System (BioRad). After the amplification phase, a dissociation curve was obtained in order to ensure that there was only one product amplified. All reactions were run in triplicate. Statistical analysis of relative expression results was carried out with the REST software tool (Pfaffl et al., 2002). Results are given as copies of RNA per 1000 copies of U6. Primer sequences for the mRNAs are indicated in the Table S2.

2.6. Prediction of miRNA binding sites

To predict miR-8-3p and miR-8-5p binding sites in the 3′-UTR of atrophin with the highest and comparable reliability, we used the following algorithms and parameter sets. RNAhybrid (http://bibiserv.techfak.uni-bielefeld.de/rnahybrid/) (Rehmsmeier et al., 2004), with a distribution probability of parameter $\xi = 1.98$ and $\Theta = 1.16$; miRanda (http://www.microrna.org) (Enright et al., 2003), with a score threshold of 100; PITA (http://genie.weizmann.ac.il/index.html) (Kertesz et al., 2007), with the seed limitation between 5 and 8; and miRiam (http://ferrolab.dmi.unict.it/miriam.html) (Lagana et al., 2010), with the highest sensibility parameters of the setting.

2.7. Luciferase assay to assess the occurrence of miR-8-3p and miR-8-5p sites

Luciferase reporters were generated by PCR amplification of a DNA fragment corresponding to the 3′UTR of the atrophin transcript from pSTBlue-1 vector (Novagen) using the primers: Atroph-Fwd and Atroph-Rev (primer sequences indicated in the Table S3), and cloned under the control of the tubulin promoter downstream of the Firefly luciferase coding region between the SpeI and XhoI sites of plasmid pJ-Luc described elsewhere (Rehwinkel et al., 2005). All PCR fragments were cloned SpeI-XhoI in the pJ-Luc vector and confirmed by sequencing. To study the expression of miR-8, a fragment of 272 bp encompassing the miR-8 hairpin was amplified by PCR with the primers: miR-8-Fwd and miR-8-Rev (primer sequences indicated in the Table S3) from *D. melanogaster* genomic DNA and cloned in vector pAc5.1 (Actin Promoter)

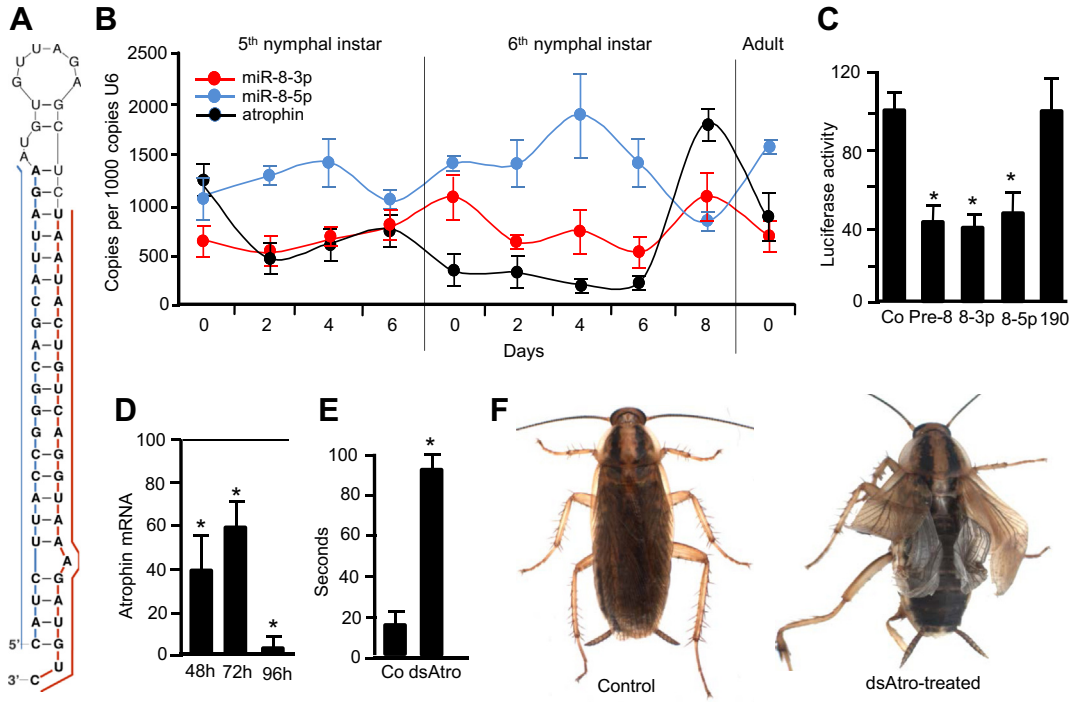

Fig. 1. MiR-8 and atrophin in *B. germanica*. (A) Hairpin structure of the miR-8 precursor. (B) Expression patterns of miR-8-3p, miR-8-5p and atrophin mRNA in the two last nymphal instars and the first day of adult; data are expressed as miRNA or mRNA copies per 1000 copies of U6, and each point represent three biological replicates. (C) Luciferase activity for a reporter transgene containing the 3′UTR of *B. germanica* atrophin mRNA, either alone (Co), or coexpressed with the miR-8 precursor (Pre-8) or incubated with single strand RNAs corresponding to miR-8-3p (8-3p), miR-8-5p (8-5p) or miR-190-3p (190), the later used as negative control. (D) Depletion of atrophin mRNA by RNAi; freshly emerged last instar female nymphs were treated with dsRNA for atrophin (dsAtro) or with dsMock, and mRNA levels were determined 48, 72 and 96 h later using qRT-PCR and U6 as a reference; data represent 3 biological replicates and are normalized against control females (reference value corresponding to dsMock treatments = 1); the asterisk indicates statistically significant differences with respect to controls ($p < 0.05$) according to the REST software tool (Pfaffl et al., 2002). (E) Effects of RNAi depletion of atrophin on the time spent climbing to the top of a 10 cm-high glass jar; freshly emerged last instar female nymphs were treated with dsAtro, and the observation was carried out 48 h later; controls (Co) received an equivalent treatment with dsMock; data represent 12 biological replicates; the asterisk indicates statistically significant differences with respect to controls (*t*-test, $p < 0.01$). (F) Adult phenotype of the specimens that were treated with dsAtro as freshly emerged last instar nymphs, showing defects in the extension of wings and in the shape of the leg, especially the hind tibiae; a control adult is showed for comparison.

between the EcoRI and XhoI sites. pAc5.1 plasmid expressing Renilla luciferase served as transfection control. S2 cells were transfected in 24-well plates with Cellfectin (Invitrogen) following the manufacturer's instructions. Transfections were performed in triplicate and contained per well: 100 ng of Firefly luciferase reporter plasmid, 0.5 μg of the Renilla luciferase transfection control plasmid and, in a first set of experiments we transfected 1 μg of miRNA expression plasmid or empty vector, and in a second set of experiments we transfected single-strand RNA (ssRNA) oligo with the sequence of miR-8-3p or miR-8-5p (SIGMA) at a concentration of 500 ng/μL. MiR-190-3p used at the same conditions served as negative control. Dual-luciferase assays (Promega) were performed 48–60 h after transfection according to the manufacturer's instructions.

2.8. mRNA depletion by RNAi

Procedures for RNAi experiments were as described previously (Gomez-Orte and Belles, 2009). To deplete atrophin, we prepared a dsRNA encompassing a 268 bp region, using the primers AtroFwF and AtroRvF (primer sequences indicated in the Table S4). The dsRNA was injected at a dose of 2.5 μg in *B. germanica* females in freshly emerged sixth (last) instar nymphs. Expression of atrophin, miR-8-5p and miR-8-3p was examined on whole body extracts 48, 72 and 96 h later by qRT-PCR. Depletion of AGO1 was carried out with a dsRNA encompassing a 249 bp region, using the primers AGO1Fw and AGO1Rv (primer sequences indicated in the Table S3). To deplete AGO2, we used a dsRNA encompassing a 437 bp region, using the primers: Arg2_Fw_1 and Arg2_Rv_1 (primer sequences indicated in the Table S3). dsAGO1 and dsAGO2 were injected at a dose of 0.5 μg and 2.5 μg, respectively in *B. germanica* females in freshly emerged fifth (penultimate) instar nymphs. Expression of AGO1, AGO2, miR-8-5p and miR-8-3p was examined on whole body extracts in the freshly emerged last instar nymphs by qRT-PCR. A 307-bp sequence from *Autographa californica* nucleopoyhedrovirus (Accession number K01149, from nucleotide 370–676) was used as control dsRNA (dsMock) in all cases, injected at the same dose and days of the specific treatments.

2.9. Depletion of miRNAs

Depletion of the miRNAs was carried out by abdominal injection of LNA specific anti-miRs: miRCURY LNA™ microRNA Inhibitor (Exiqon), at a concentration of 50 μM, in freshly emerged last instar female nymphs of *B. germanica*. Controls were injected with miRCURY LNA™ microRNA Inhibitor Control A (Exiqon) at the same dose and age. Expression of atrophin, miR-8-3p and miR-8-5p was determined by qRT-PCR on whole body extracts 2, 4, 6 and 24 h after the treatment. Freshly emerged sixth instar nymphs were treated with 1 μL of a 50 μM solution of LNA-miR-8-3p or LNA-miR-8-5p.

2.10. Behaviour experiments

Two days after the injection of dsAtro, we anaesthetized the cockroaches during 30 s with a constant flux of carbon dioxide, and

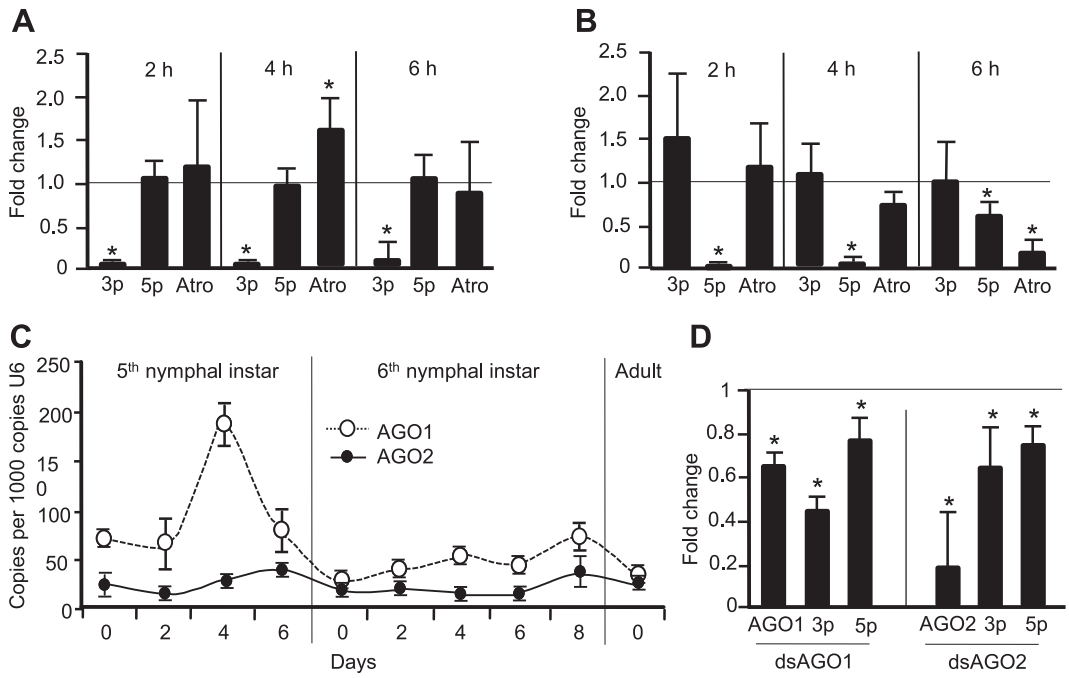

Fig. 2. Effects of miR-8-3p and miR-8-5p depletion and the role of AGO1 and AGO2 in *B. germanica*. (A) Effect of the depletion of miR-8-3p; freshly emerged last instar female nymphs were treated with LNA specific anti-miR-8-3p, whereas controls received an equivalent treatment with LNA microRNA Inhibitor Negative Control; levels of miR-8-3p, miR-8-5p and atrophin mRNA were determined 2, 4 and 6 h after the treatment; data represent 3 biological replicates and are normalized against control females data (reference value = 1); the asterisk indicates statistically significant differences with respect to controls ($p < 0.05$) according to the REST software tool (Pfaffl et al., 2002). (B) Effect of the depletion of miR-8-5p; experimental details were equivalent as those described in A. (C) Expression patterns of AGO1 and AGO2 mRNAs in the two last nymphal instars and the first day of adult; data show miRNA copies per 1000 copies of U6, and each point represent three biological replicates. (D) Effects of RNAi depletion of AGO1 and AGO2 mRNA on miR-8-3p (3p) and miR-8-5p (5p) levels; freshly emerged last instar female nymphs were treated with dsAGO1 or dsAGO2 (or dsMock), and observations were carried out just after emerging to the sixth instar using qRT-PCR and U6 as a reference; data are expressed as miRNA copies per 1000 copies of U6, each point represent three biological replicates and is normalized against the control females (reference value reference value corresponding to dsMock treatments = 1); the asterisk indicates statistically significant differences with respect to controls ($p < 0.05$) according to the REST software tool (Pfaffl et al., 2002).

we placed them into a glass jar of 17 cm high and 10 cm diameter. The top 10 cm of the jar were covered with a black plastic, and we placed a source of light 21 cm from the jar and 5 cm from the base. Cockroaches started to wake up 2–3 min after the anaesthesia and we measured the time that they spent climbing to the top of the jar to become hidden in the dark. Control individuals were studied following the same protocol.

3. Results

3.1. MiR-8 in B. germanica

Cloning of the precursor of miR-8 (pre-miR-8) gave a 59 bp sequence that folded into the characteristic hairpin structure of a miRNA precursor (Fig. 1A). Alignment of the miR-8 precursor in different arthropod species showed that the regions corresponding to miR-8-5p and miR-8-3p are highly conserved (Fig. S1). These regions maintain a high level of conservation, not only in arthropods but also in metazoans in general, where five miRNAs from the same family (miR-200a, miR-200b, miR-200c, miR-429 and miR-141) are orthologues of miR-8 (Fig. S2). The expression of miR-8-3p and miR-8-5p in the two latest instar nymphs (fifth and sixth) and in freshly ecdysed adults of *B. germanica* females shows similar expression patterns, except at the very late stage of each instar (day 6 of fifth instar, day 8 of sixth instar) and the adult stage (Fig. 1B).

3.2. Atrophin: a target for miR-8 in B. germanica

In *D. melanogaster*, miR-8-3p regulates transcript levels of atrophin (Karres et al., 2007). To investigate whether *B. germanica* atrophin would also be a target not only for miR-8-3p but also to miR-8-5p, we cloned a 1820 bp cDNA corresponding to a partial sequence of the atrophin orthologue of *B. germanica* that included 461 amino acids of the 3′ region of the ORF and the complete 3′UTR, which was confirmed by 3′ RACE (GenBank accession number: HF912426). We then predicted binding sites for miR-8-3p and miR-8-5p in the 3′-UTR of atrophin using RNAhybrid, miRanda, PITA and miRiam algorithms. For each algorithm we used the set of parameters appropriate to obtain the highest scored sites with comparable reliability, and we obtained a collection of modestly scored sites for miR-8-5p (1 using RNAhybrid, 4 with miRanda, 1 with PITA and 2 with miRiam) and for miR-8-3p (1 with RNAhybrid, 5 with miRanda, 2 with PITA and 1 with miRiam), most of which being non-coincident (Table S5).

Given the considerable diversity and incongruence of the sites predicted by the different algorithms, which covered practically the entire 3′UTR region of atrophin, we simply assessed whether this region contained functional sites for miR-8-3p and for miR-8-5p, without undertaking mutational analysis to localize them. To this purpose, we linked the atrophin entire 3′UTR to a luciferase reporter gene and coexpressed this construct in Drosophila S2 cells with the *D. melanogaster* miR-8 precursor (which leads to the production of mature sequences identical to those of *B. germanica* miR-8-5p and miR-8-3p). Coexpression with the miR-8 precursor reduced luciferase enzyme activity to ca. 60% of that of the control (Fig. 1C), a reduction that is similar to that reported by Karres et al. (2007) in *D. melanogaster*. A comparable reduction was observed in response to single-strand RNA oligonucleotides of miR-8-3p and miR-8-5p respectively added to the medium (Fig. 1C). These results indicated that the 3′UTR of

B. germanica atrophin mRNA contains functional binding sites for miR-8-5p and miR-8-3p.

3.3. Atrophin deficiency affects motor and molting behaviour in B. germanica

The functions of atrophin in *B. germanica* were subsequently characterized. Atrophin mRNA levels in the two last nymphal instars and in freshly ecdysed adults of *B. germanica* females showed a relatively stable pattern until the last day of the final nymphal instar, where they formed a prominent peak, which coincides with the moment where the levels of miR-8-5p are the lowest, and those of miR-8-3p the highest (Fig. 1B). In *D. melanogaster*, high levels of atrophin led to significant apoptosis in brain tissues, which impaired motor coordination and caused defects in the ecdysis (Karres et al., 2007). To assess the possible functions of atrophin in *B. germanica*, atrophin mRNA levels were depleted by RNAi. Significantly reduced atrophin mRNA levels were observed in freshly emerged sixth instar nymphs at 24, 48 and 96 h after treatment with a specific dsRNA (dsAtro), compared to levels observed in controls (equivalently treated with a dsRNA corresponding to an alien sequence from *A. californica* nucleopolyhedrovirus: dsMock) (Fig. 1D). Two days after the dsAtro treatment, the specimens exhibited obvious motor problems, as shown by an extended time (90 s on average) that they required to climb to the top of a 17 cm-high glass jar, in comparison to dsMock-treated controls (15 s; see Fig. 1E). This suggests that atrophin activity must be tightly regulated as deviations elicit motor coordination problems. Our dsAtro-treated specimens were able to molt to the adult stage, but the process of shedding the exuvia was slower and less efficient than that of controls, and the molted specimens showed mechanical defects in the forms of twisted and curved legs and partially extended and wrinkled wings (Fig. 1F).

3.4. MiR-8-5p and miR-8-3p affect atrophin mRNA levels

To assess whether atrophin mRNA levels are affected by miR-8-5p and miR-8-3p, the two miRNAs were suppressed with specific LNA anti-miRs administered to freshly-emerged sixth instar nymphs. In comparison with controls (treated with LNA microRNA Inhibitor Control A), specimens treated with LNA-anti-miR-8-3p showed levels of miR-8-3p reduced by more than 95% at 2, 4 and 6 h after the treatment, although at 6 h a very modest recovery was observed (Fig. 2A). The specificity of the treatment was demonstrated by the unaffected levels of miR-8-5p. The levels of atrophin mRNA were unstable, from a tendency to increase at 2 h, a significant increase at 4 h, and a return to practically basal levels at 6 h (Fig. 2A). Tendency towards increasing the target mRNA levels when the targeting miRNA is suppressed is the response observed in miRNA action associated to AGO1-RISC mechanisms that leads to target blocking and translational repression. A recent example of this has been reported in the silk moth, *Bombyx mori*, where LNA suppression of miR-8-3p led to an increase of mRNA levels of the NPV immediate-early gene, considered to be one of its targets (Singh et al., 2012). In our experiments, equivalent treatments with LNA-anti-miR-8-5p resulted in dramatic and specific suppression (more than 95%) of miR-8-5p, as measured at 2 and 4 h after the treatment, but a significant recovery (reaching more than 50% of control levels) was observed at 6 h (Fig. 2B). In this case, the levels of atrophin mRNA were apparently unaffected at 2 h, tended to decrease at 4 h, and were significantly lower (reduced by more than 85%) than controls at 6 h, a decrease that occurred in parallel with the recovery of miR-8-5p levels (Fig. 2B). The effects of miR-8-5p depletion upon atrophin mRNA are difficult to interpret. The whole data might suggest that atrophin mRNA levels decreased when miR-8-5p is depleted; however, careful comparison of the respective dynamics of miR-8-5p and atrophin during the experiment indicates that the tendency to recover of miR-8-5p between 4 and 6 h is parallelled by a tendency to decrease atrophin mRNA levels during the same interval. This suggests that miR-8-5-p also have antagonistic effects upon atrophin, which could be mediated, however, by mechanisms different to those operating in the case of miR-8-3p.

3.5. The role of AGO1 and AGO2

We have speculated about different modes of action of miR-8-3p and miR-8-5p upon atrophin mRNA, and wondered whether they could be mediated by differential loading with AGO1 or AGO2 in the RISC complex. With the aim of gaining more evidence on the sorting of miR-8-3p and miR-8-5p to AGO1 or to AGO2, we investigated these two proteins in *B. germanica*. As a first step, we cloned a 2688 bp cDNA corresponding to a partial sequence of the AGO1 orthologue of *B. germanica* (GenBank accession number: HF912424), and a 2895 bp cDNA corresponding to a partial sequence of the AGO2 orthologue (GenBank accession number: HF912425). The predicted translation rendered two protein sequences, one with 896 amino acids (AGO1) and the other with 993 (AGO2), which contained the PAZ and PIWI domains that are typical of AGO proteins. We then determined the expression pattern of both mRNAs in the two latest instar nymphs (fifth and sixth) and in freshly ecdysed adults of *B. germanica* females, which was quite stable except for AGO2 which showed a peak during the 4th day of the fifth nymphal instar (Fig. 2C). Subsequently, we studied the effects of AGO1 and AGO2 suppression by RNAi on miR-8-3p and miR-8-5p levels by administering the respective dsRNAs (dsAGO1 and dsAGO2) on freshly emerged fifth instar nymphs. With respect to dsAGO1, all specimens treated with 3.75 μg ($n = 10$) or 1.5 μg ($n = 10$) died during the next molt. At a dose of 0.5 μg, 67.5% (54 out of 80 dsAGO1-treated specimens) also died during the next molt. The results presented here are based on the survivors of this experiment. With dsAGO2, we used a dose of 2.5 μg, which was not lethal. Treatments with 0.5 μg of dsAGO1 resulted in a moderate suppression of AGO1 mRNA levels (ca. 30% reduction), but this was sufficient to significantly affect levels of miR-8-3p (ca. 60% reduction) and miR-8-5p (ca. 25% reduction; Fig. 2D). Treatments with 2.5 μg of dsAGO2 more efficiently suppressed AGO2 mRNA levels (ca. 80% reduction), and affected levels of miR-8-3p (ca. 30% reduction) and miR-8-5p (ca. 25% reduction; Fig. 2D), in comparison with insects treated with dsMock.

Under the assumption that depletion of AGO1 or AGO2 results in degradation of the associated miR-8 strand, then these results suggest that miR-8-3-p predominantly binds to AGO1 and, to a minor extent, to AGO2, whereas miR-8-5p binds to a moderate extent to both AGO1 and AGO2. In general, miRNA sequences with uridine (U) as their first nucleotide tend to bind to AGO1 whereas those beginning with cystidine (C) tend to bind to AGO2 (Ghildiyal et al., 2010). In *D. melanogaster*, moreover, Czech et al. (2009) have shown that miR-8-3p (which begins with U) binds predominantly to AGO1 (80%) in the RISC (and 20% to AGO2), whereas miR-8-5p (which begins with C) preferentially binds to AGO2 (60%), but also to AGO1 (40%). The results obtained in *B. germanica* are in agreement with these antecedents.

4. Discussion

The data obtained from *B. germanica* point to a finely-tuned posttranscriptional regulation of atrophin mRNA levels by the interplay of miR-8-3p and miR-8-5p, which would act through different mechanisms possibly mediated by differentially binding

to AGO1 and AGO2 in the corresponding RISC. This is suggested by the quantitative changes of expression observed in these four players and atrophin when the abundance of one of them is changed experimentally. The results suggest that miR-8-3p would preferentially bind to AGO1 in the RISC (and to a lower extent to AGO2), whereas miR-8-5p would bind practically equally to AGO1 and AGO2, as happens in *D. melanogaster* (Czech et al., 2009). Differential sorting is important because miRNAs loading in AGO1-RISC follow the conventional miRNA pathway leading to blocking and translational repression of the target mRNA, whereas miRNAs loading in AGO2-RISC follow a pathway optimized for target mRNA degradation (Forstemann et al., 2007). Indeed, the relative catalytic constant of AGO2 is 43-fold higher than that of AGO1, thus, the miR-8 strands that bind to AGO2 would more actively degrade atrophin mRNA than those binding to AGO1 (Forstemann et al., 2007).

We are aware that this interpretation is a qualitative and a rather simplistic approximation to the complex interactions that are likely to occur, not only of miRNAs with AGO proteins but also of the miRNA-AGO-RISC with the target mRNA, which possess sites for both miR-8-3p and miR-8-5p and the interaction of one AGO-RISC in one site may affect interactions with other sites. Above all, the results suggest that the two strands of the same miRNA precursor cooperate to achieve a finely-tuned regulation of a given mRNA target. In this case, the mRNA corresponds to atrophin, a protein that ensures proper neural functioning and neuromotor coordination in such a fine way that minor deviations from the normal pattern, such as those induced in our experiments, elicit serious motor malfunctions. Motor malfunctions were noticed not only in the climbing experiments, but can be also inferred from the deformations observed in the legs and wings of the adults emerging from nymphs with RNAi-depleted atrophin. In *D. melanogaster*, high levels of atrophin resulting from miR-8 mutations led to significant apoptosis in brain tissues and defects in the adult after the imaginal ecdysis, like deformed hindlegs and wrinkled wings (Karres et al., 2007). Moreover, direct mutations of atrophin in *D. melanogaster* cause leg patterning defects (Erkner et al., 2002; Wang et al., 2006) and ectopic vein formation in the wings (Charroux et al., 2006). In *B. germanica*, direct depletion of atrophin by RNAi appears specifically associated to impaired motor coordination, given that the phenotype observed did not include ectopic veins in the wings and defects in leg patterning. Indeed, the resulting phenotype seems rather related to mechanical problems derived from an improper ecdysis. These results and the prominent peak of atrophin expression occurring at the end of the last nymphal stage, just before the imaginal molt, suggest that higher levels of atrophin are crucial for neuromotor coordination during the imaginal ecdysis, when shedding out the exuvia becomes a process more complex than in a nymphal moult due to the apparition of new structures, particularly the wings and tegmina.

Acknowledgements

Support for this research was provided by the Spanish Spanish Ministry of Science and Innovation (grant CGL2008-03517/BOS to X.B.; BFU2010-21123 and CSD2007-00008 to M.M.), by FEDER funds, and by the CSIC (grant 2010TW0019, from the Formosa program, to X.B. and a predoctoral fellowship to M.R. from the JAE program). M.M. is an ICREA Research Professor.

Appendix A. Supplementary data

Supplementary data related to this article can be found at http://dx.doi.org/10.1016/j.ibmb.2013.08.003.

References

Bartel, D.P., 2004. MicroRNAs: genomics, biogenesis, mechanism, and function. Cell 116, 281–297.
Belles, X., Cristino, A.S., Tanaka, E.D., Rubio, M., Piulachs, M.-D., 2012. Insect microRNAs: from molecular mechanisms to biological roles. In: Gilbert, L.I. (Ed.), Insect Molecular Biology and Biochemistry. Elsevier-Academic Press, Amsterdam, pp. 30–56.
Berezikov, E., Robine, N., Samsonova, A., Westholm, J.O., Naqvi, A., Hung, J.H., Okamura, K., Dai, Q., Bortolamiol-Becet, D., Martin, R., Zhao, Y., Zamore, P.D., Hannon, G.J., Marra, M.A., Weng, Z., Perrimon, N., Lai, E.C., 2011. Deep annotation of *Drosophila melanogaster* microRNAs yields insights into their processing, modification, and emergence. Genome Res. 21, 203–215.
Cristino, A.S., Tanaka, E.D., Rubio, M., Piulachs, M.D., Belles, X., 2011. Deep sequencing of organ- and stage-specific microRNAs in the evolutionarily basal insect *Blattella germanica* (L.) (Dictyoptera, Blattellidae). PLoS One 6, e19350.
Czech, B., Zhou, R., Erlich, Y., Brennecke, J., Binari, R., Villalta, C., Gordon, A., Perrimon, N., Hannon, G.J., 2009. Hierarchical rules for argonaute loading in *Drosophila*. Mol. Cell 36, 445–456.
Charroux, B., Freeman, M., Kerridge, S., Baonza, A., 2006. Atrophin contributes to the negative regulation of epidermal growth factor receptor signaling in *Drosophila*. Dev. Biol. 291, 278–290.
Christodoulou, F., Raible, F., Tomer, R., Simakov, O., Trachana, K., Klaus, S., Snyman, H., Hannon, G.J., Bork, P., Arendt, D., 2010. Ancient animal microRNAs and the evolution of tissue identity. Nature 463, 1084–1088.
Ebert, M.S., Sharp, P.A., 2012. Roles for microRNAs in conferring robustness to biological processes. Cell 149, 515–524.
Enright, A.J., John, B., Gaul, U., Tuschl, T., Sander, C., Marks, D.S., 2003. MicroRNA targets in *Drosophila*. Genome Biol. 5, R1.
Erkner, A., Roure, A., Charroux, B., Delaage, M., Holway, N., Core, N., Vola, C., Angelats, C., Pages, F., Fasano, L., Kerridge, S., 2002. Grunge, related to human Atrophin-like proteins, has multiple functions in *Drosophila* development. Development 129, 1119–1129.
Forstemann, K., Horwich, M.D., Wee, L., Tomari, Y., Zamore, P.D., 2007. *Drosophila* microRNAs are sorted into functionally distinct argonaute complexes after production by dicer-1. Cell 130, 287–297.
Ghildiyal, M., Xu, J., Seitz, H., Weng, Z., Zamore, P.D., 2010. Sorting of *Drosophila* small silencing RNAs partitions microRNA* strands into the RNA interference pathway. RNA 16, 43–56.
Gomez-Orte, E., Belles, X., 2009. MicroRNA-dependent metamorphosis in hemimetabolan insects. Proc. Natl. Acad. Sci. U. S. A. 106, 21678–21682.
Griffiths-Jones, S., Saini, H.K., van Dongen, S., Enright, A.J., 2008. miRBase: tools for microRNA genomics. Nucleic Acids Res. 36, D154–D158.
Gruber, A.R., Lorenz, R., Bernhart, S.H., Neubock, R., Hofacker, I.L., 2008. The Vienna RNA websuite. Nucleic Acids Res. 36 (suppl 2), W70–W74. http://dx.doi.org/10.1093/nar/gkn188.
Karres, J.S., Hilgers, V., Carrera, I., Treisman, J., Cohen, S.M., 2007. The conserved microRNA miR-8 tunes atrophin levels to prevent neurodegeneration in *Drosophila*. Cell 131, 136–145.
Kertesz, M., Iovino, N., Unnerstall, U., Gaul, U., Segal, E., 2007. The role of site accessibility in microRNA target recognition. Nat. Genet. 39, 1278–1284.
Kim, V.N., Han, J., Siomi, M.C., 2009. Biogenesis of small RNAs in animals. Nat. Rev. Mol. Cell Biol. 10, 126–139.
Lagana, A., Forte, S., Russo, F., Giugno, R., Pulvirenti, A., Ferro, A., 2010. Prediction of human targets for viral-encoded microRNAs by thermodynamics and empirical constraints. J. RNAi Gene Silencing: Int. J. RNA Gene Target. Res. 6, 379–385.
Lee, R.C., Feinbaum, R.L., Ambros, V., 1993. The *C. elegans* heterochronic gene lin-4 encodes small RNAs with antisense complementarity to lin-14. Cell 75, 843–854.
Okamura, K., Liu, N., Lai, E.C., 2009. Distinct mechanisms for microRNA strand selection by *Drosophila* Argonautes. Mol. Cell 36, 431–444.
Okamura, K., Phillips, M.D., Tyler, D.M., Duan, H., Chou, Y.T., Lai, E.C., 2008. The regulatory activity of microRNA* species has substantial influence on microRNA and 3' UTR evolution. Nat. Struct. Mol. Biol. 15, 354–363.
Pfaffl, M.W., Horgan, G.W., Dempfle, L., 2002. Relative expression software tool (REST) for group-wise comparison and statistical analysis of relative expression results in real-time PCR. Nucleic Acids Res. 30, e36.
Rehmsmeier, M., Steffen, P., Hochsmann, M., Giegerich, R., 2004. Fast and effective prediction of microRNA/target duplexes. RNA 10, 1507–1517.
Rehwinkel, J., Behm-Ansmant, I., Gatfield, D., Izaurralde, E., 2005. A crucial role for GW182 and the DCP1:DCP2 decapping complex in miRNA-mediated gene silencing. RNA 11, 1640–1647.
Singh, C.P., Singh, J., Nagaraju, J., 2012. A baculovirus-encoded MicroRNA (miRNA) suppresses its host miRNA biogenesis by regulating the exportin-5 cofactor Ran. J. Virol. 86, 7867–7879.
Wang, L., Rajan, H., Pitman, J.L., McKeown, M., Tsai, C.C., 2006. Histone deacetylase-associating Atrophin proteins are nuclear receptor corepressors. Genes Dev. 20, 525–530.
Wang, L., Tsai, C.C., 2008. Atrophin proteins: an overview of a new class of nuclear receptor corepressors. Nucl. Recept. Signal. 6, e009.
Yang, J.S., Phillips, M.D., Betel, D., Mu, P., Ventura, A., Siepel, A.C., Chen, K.C., Lai, E.C., 2011. Widespread regulatory activity of vertebrate microRNA* species. RNA 17, 312–326.

SUPPLEMENTARY INFORMATION

Regulation of atrophin by both strands of the mir-8 precursor

Mercedes Rubio[1], Raul Montañez[1], Lidia Perez[2], Marco Milan[2], Xavier Belles[1*]

Contents

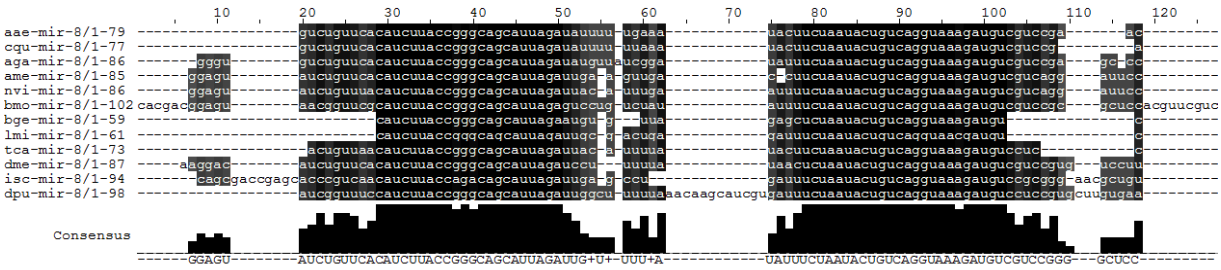

Fig. S1. Alignment of the miR-8 precursor of *Blattella germanica* with mir-8 homologs in other arthropod species. Insects: *Aedes aegypti* (aae), *Anopheles gambiae* (aga), *Apis mellifera* (ame), *Blattella germanica* (bge), *Bombyx mori* (bmo), *Culex quinquefasciatus* (cqu), *Drosophila melanogaster* (dme), *Locusta migratoria* (lmi), *Nasonia vitiprennis* (nvi), *Tribolium castaneum* (tca); crustacean: *Daphnia pulex* (dpu); arachnid: *Ixodes scapularis* (isc).

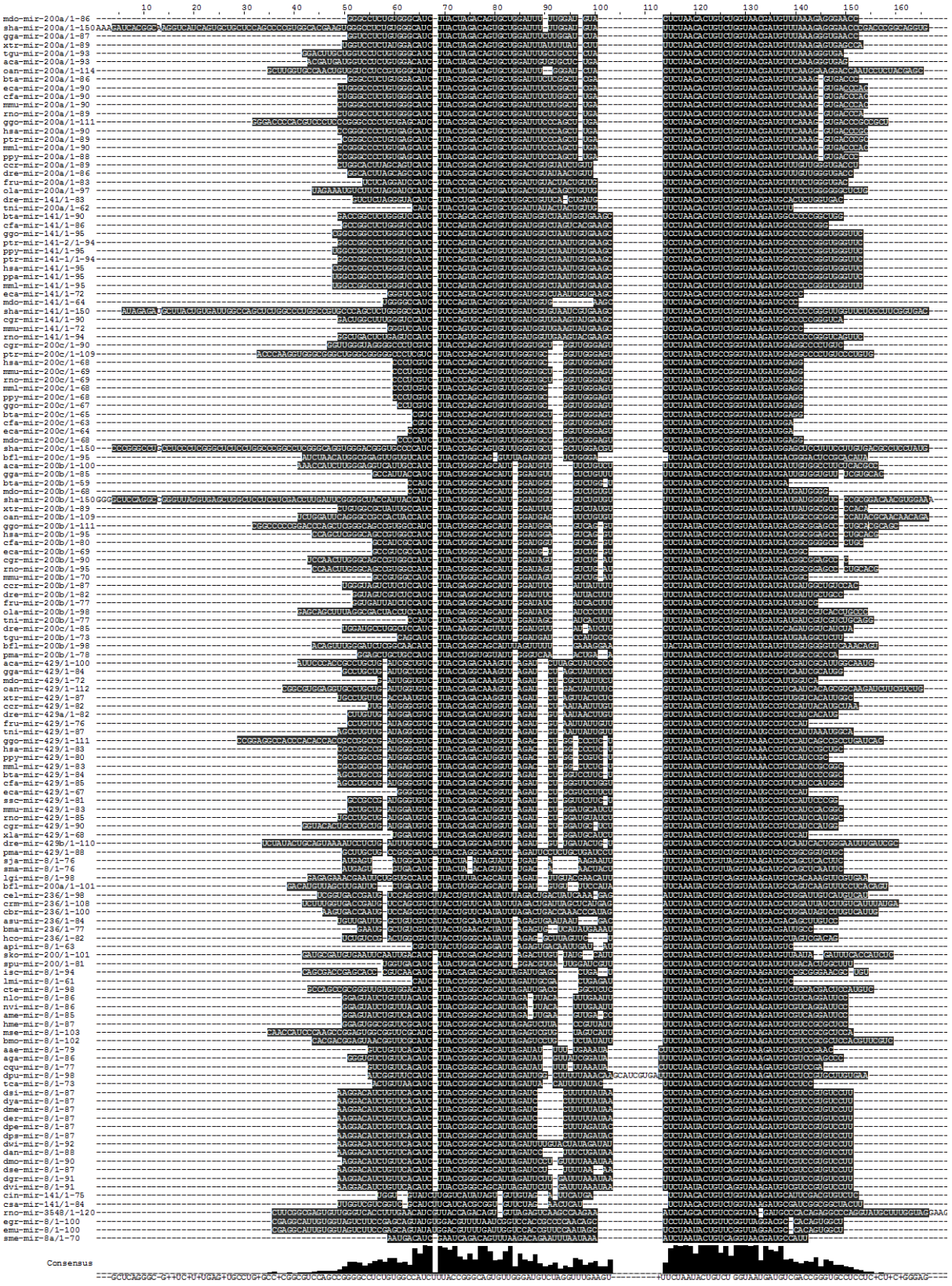

Fig. S2. Alignment of the miR-8 precursor (or homolog miRs) of metazoan species of miRBase (release 18).

Table S1

Primer sequences used to obtain the mRNA sequence of atrophin, argonaute 1 and argonaute 2 in *Blattella germanica*.

Gene	Primer name	Primer sequence
Atrophin	AtroFwF	5'-ACGGAGTCAGAGTGCTATTTT-3'
	AtrophRv	5'-GCATGYGTATGNGCGTG-3'
	AtrophFw_2	5'-GAGTATGCKMGACCACATGC-3'
	BgAtroFw	5'-CAGCAGCTCAGCTAGAAGCA-3'
	BgAtroFw_2	5'-CCAGAGTACCATGCGCAC-3'
	BgAtroRv	5'-CAAGCTGACAGCAGAGTTCG-3'
Argonaute 1	Ago1 Fw2	5'-ATGTCTCCCGTTGGGCAGC-3'
	Ago1Rv2	5'-ATGGTCTAACGGACTGATG-3'
	Ago1 Fw3	5'-GCCAGACTCTCACAACTTGT-3'
	Ago1 Rv3	5'-CACATGCAAGAACTGTCCTTC-3'
	Ago1 Fw4	5'-GAAGGACAGTTCTTGCATGTG-3'
	Ago1 Rv4	5'-GCTCTTGACCAACTTGAAGACA-3'
Argonaute 2	Ago2 Fw	5'-GGCTACAATCAGAGCCCCTA-3'
	Ago2 Rv	5'-GCATAGTAACCCGTCCCCTA-3'
	Ago2 Fwcontig1	5'-CATTTCAGACCGCTGCTACA-3'
	Ago2 Rvcontig1	5'-GATGGGTCACATCAGCTCCT-3'
	Ago2 Fwcontig2	5'-TCAAAAATACCACCGGCTATG-3'
	Ago2 Rvcontig3	5'-AAACATGAAATAACGACTAAGGAGAAA-3'
	Ago2 5' Fw_1	5'-CACTCCCGGTGGACGTTCTC-3'
	Ago2 5’ Rv_1	5'-CTTCCATGGCATACCTGAGC-3'
	Ago2 Fw2	5'-GTCTCCAGCACCGGAAAAG-3'
	Ago2 Rv2	5'-ACAACTTTTTGTCCCAGCAAG-3'

Table S2

Primer sequences used for quantification of atrophin, argonaute 1 and argonaute 2 in *Blattella germanica* by qRT-PCR.

Gene	Primer name	Primer sequence
Atrophin	RTAtro Fw	5'-GGTTACCTCCCCAGTGCATA-3'
	RTAtro Rv	5'-CCAAATGCTCCAATTCCAGT-3'
Argonaute 1	RTAgo1 Fw	5'-CACTCACTGTGGGACCATGA-3'
	RTAgo1 Rv	5'-CTCCTCGTCACATTGCACAC-3'
Argonaute 2	RTAgo2 Fw	5'-GCAAGGACCATGCAGAGAAT-3'
	RTAgo2 Rv	5'-AGACTGATGCGATGCAGTGA-3'

Table S3

Primer sequences used in the luciferase experiments to assess the occurrence of functional binding sites for miR-8-3p and miR-8-5p in the 3'UTR of *Blattella germanica* atrophin mRNA.

Primer name	Primer sequence
Atroph-Fwd	5'-GGACTAGTATTAGACACTCGACTGCCATC-3'
Atroph-Rev	5'-CCGCTCGAGTGTCTTCTAGAACAGAAACTAAAG-3'
miR-8-Fwd	5'-GGAATTCAATGGAATACCGAATCTTGCT-3'
miR-8-Rev	5'-ATGCTCGAGTTGTCTTCGCATTATCCAC-3'

Table S4

Primer sequences used to prepare the dsRNA to deplete atrophin (AtroFwF and AtroRvF), Argonaute 1 (Ago1Fw and Ago1Rv) and argonaute 2 (Arg2_Fw_1 and Arg2_Rv_1) in *Blattella germanica* by RNAi.

Gene	Primer name	Primer sequence
Atrophin	AtroFwF	5'-ACAGGAGTCAGAGTGCTATTTT-3'
	AtroRvF	5'-TATGGAGAAGTGATAGTTTCAATA-3'
Argonaute 1	Ago1Fw	5'-CCTCTTCCCATAGGAAATGACA-3'
	Ago1Rv	5'-TCCATCAGGAGATGAGAAAAA-3'
Argonaute 2	Arg2_Fw_1	5'-AAGGGCTGGCTACAATCAGA-3'
	Arg2_Rv_1	5'-AGCAGTCTTTGAACCGAGGA-3'

Table S5

Prediction of miRNA binding sites for miR-8-5p and miR-8-3p in the 3'-UTR of *Blattella germanica* atrophin mRNA using different algorithms. RNAhybrid (http://bibiserv.techfak.uni-bielefeld.de/rnahybrid/) was used with a distribution probability of parameter ξ=1.98 and Θ=1.16; miRanda (http://www.microrna.org) with a score threshold of 100; PITA (http://genie.weizmann.ac.il/index.html) with the seed limitation between 5 and 8; and miRiam (http://ferrolab.dmi.unict.it/miriam.html) with the highest sensibility parameters of the setting. Mfe: minimum free energy.

Algorithm	**miRNA**	**Start**	**End**	**Mfe** (kcal/mol)
RNAhybrid	miR-8-5p	267	288	-21.7
	miR-8-3p	297	348	-19.7
miRanda	miR-8-5p	69	88	-6.16
	miR-8-5p	165	186	-3.27
	miR-8-5p	193	214	-0.30
	miR-8-5p	394	415	-1.21
	miR-8-3p	45	68	-12.11
	miR-8-3p	64	86	-6.75
	miR-8-3p	227	251	-8.66
	miR-8-3p	269	291	-5.62
	miR-8-3p	325	347	-5.54
PITA	miR-8-5p	181	186	-3.42
	miR-8-3p	246	251	-9.66
	miR-8-3p	339	347	-9.48
miRiam	miR-8-5p	333	356	-11.80
	miR-8-5p	368	383	-11.20
	miR-8-3p	309	333	-12.50